

Improved breakdown characteristics of monolithically integrated III-nitride HEMT–LED devices using carbon doping



Chao Liu, Zhaojun Liu, Tongde Huang, Jun Ma, Kei May Lau*

Photonic Technology Center, Department of Electronic and Computer Engineering, Hong Kong University of Science and Technology, Clear Water Bay, Kowloon, Hong Kong

ARTICLE INFO

Available online 22 October 2014

Keywords:

A1. Doping
A3. Metalorganic chemical vapor deposition
B1. Nitrides
B3. High electron mobility transistors

ABSTRACT

We report selective growth of AlGaIn/GaN high electron mobility transistors (HEMTs) on InGaIn/GaN light emitting diodes (LEDs) for monolithic integration of III-nitride HEMT and LED devices (HEMT–LED). To improve the breakdown characteristics of the integrated HEMT–LED devices, carbon doping was introduced in the HEMT buffer by controlling the growth pressure and V/III ratio. The breakdown voltage of the fabricated HEMTs grown on LEDs was enhanced, without degradation of the HEMT DC performance. The improved breakdown characteristics can be attributed to better isolation of the HEMT from the underlying conductive p-GaN layer of the LED structure.

© 2014 Elsevier B.V. All rights reserved.

1. Introduction

The past decade has witnessed tremendous progress in the development of III-nitride based light emitting diodes (LEDs) for lighting and high electron mobility transistors (HEMTs) for power applications. Combining the superior optical properties of InGaIn/GaN LEDs and excellent electrical performance of AlGaIn/GaN HEMTs can pave the way for smart lighting systems with improved system reliability and lifetime [1]. Furthermore, monolithic integration of III-nitride HEMTs and LEDs on a common platform can effectively reduce undesirable parasitics, thereby enhancing the power efficiency of the driving circuits. To date, Li et al. [2] have reported the growth of GaN-based LEDs on HEMTs, and selective removal of the LED-epi was performed for device integration. However, the LED performance was much inferior to that of discrete devices, probably due to the use of an un-optimized growth scheme on HEMTs. Recently, we demonstrated an alternative approach, selective growth of AlGaIn HEMTs on LEDs for HEMT–LED integration. The schematic of the monolithically integrated HEMT–LED structure is shown in Fig. 1. The integrated HEMT–LED devices exhibited comparable performance with respect to stand-alone HEMTs and LEDs, except for the transistor breakdown [3,4]. In our previous results, the breakdown voltage of the HEMTs was compromised by the underlying conductive p-GaN layer of the LED structure. Furthermore, limited by the low thermal budget allowance for the underlying LEDs, the

regrown GaN buffer for the upper HEMTs was kept thin, leading to insufficient isolation from the p-type GaN layer. It has been suggested that the breakdown characteristics of GaN based HEMTs can be improved by compensating the background residual donors with acceptor-like impurities (e.g. Mg, Fe or C) or defects [5–8]. However, Mg and Fe are known to have serious memory effects [5,9], which might affect the performance of the subsequently grown HEMT. Carbon, on the other hand, has a much lower diffusion coefficient and memory effect, compared to Mg and Fe. In this work, we introduced carbon doping in the regrown HEMT buffer to enhance the electrical isolation between the HEMTs and LEDs. The carbon doping concentration was varied by controlling the growth pressure and V/III ratio. The effects of the carbon doping

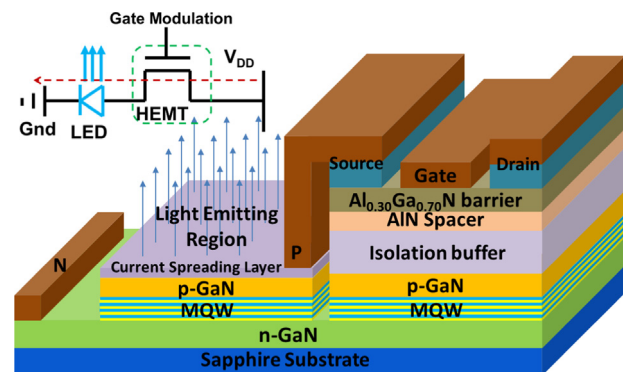


Fig. 1. Schematic of the monolithically integrated HEMT–LED structure [3].

* Corresponding author.

E-mail address: ekmlau@ust.hk (K. May Lau).

concentration on the surface morphology, breakdown characteristics, and DC performances have been investigated.

2. Experimental procedure

This specific investigation was carried out with a previously proven scheme for the integrated device [3]. Three AlGaIn/GaN

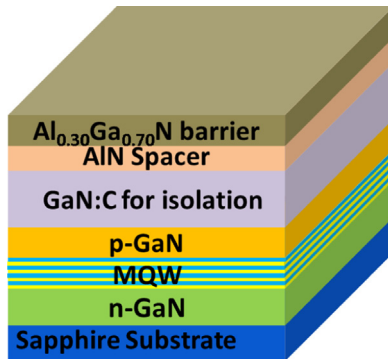


Fig. 2. Schematic of the HEMT-on-LED-epi structure.

Table 1
Growth parameters for GaN:C buffer layer of the three samples.

Sample	Temperature (°C)	Pressure (hPa)	NH ₃ flow rate (mmol/min)	TMGa flow rate (μmol/min)
A	920	200	200	180
B	920	50	200	180
C	920	50	66	180

HEMT samples were selectively grown on commercial 2-in LED wafers in an Aixtron 2400HT metal organic chemical vapor deposition (MOCVD) system, with part of the LED surface covered by a SiO₂ mask. Trimethylgallium (TMGa), trimethylaluminum (TMAI) and ammonia (NH₃) were used as Ga, Al and N sources, respectively. Nitrogen and hydrogen were used as carrier gas. Prior to growth, the LED wafers were heated up to the HEMT growth temperature of 920 °C in a H₂/N₂/NH₃ mixture ambience to protect the LED surface from decomposition. Afterwards, a 400 nm GaN:C isolation buffer and a 100 nm unintentionally doped GaN channel layer were grown, followed by a 1 nm AlN spacer layer and a 20 nm Al_{0.30}Ga_{0.70}N barrier layer. A schematic of the HEMT-on-LED epi structure is shown in Fig. 2.

To investigate the carbon doping effect, the concentration of carbon doping in the GaN:C buffer was varied by adjusting the growth parameters, as summarized in Table 1. The influence of growth conditions on carbon incorporation was compared using secondary ion mass spectrometry (SIMS) characterization. Atomic force microscopy (AFM) was used to monitor the surface morphology of the as-grown AlGaIn/GaN HEMT samples on InGaIn/GaN LEDs. After the growth and material characterization, we fabricated HEMTs with a gate width of 10 μm and a gate length of 2 μm. The distance between gate and drain was 12 μm. Device isolation of the HEMTs was performed by Cl₂-based inductively coupled plasma (ICP) etching. Afterwards, the source/drain ohmic contacts of the HEMTs were formed by e-beam evaporation of Ti/Al/Ni/Au (20/150/50/80 nm) and rapid thermal annealing (RTA) at 850 °C for 30 s in N₂. Finally, Ni/Au (20/200 nm) gate metal was deposited by e-beam evaporation.

3. Results and discussion

Fig. 3(a) shows the surface morphology of the commercial LED-epi before HEMT growth. A large density of hexagonal pits was

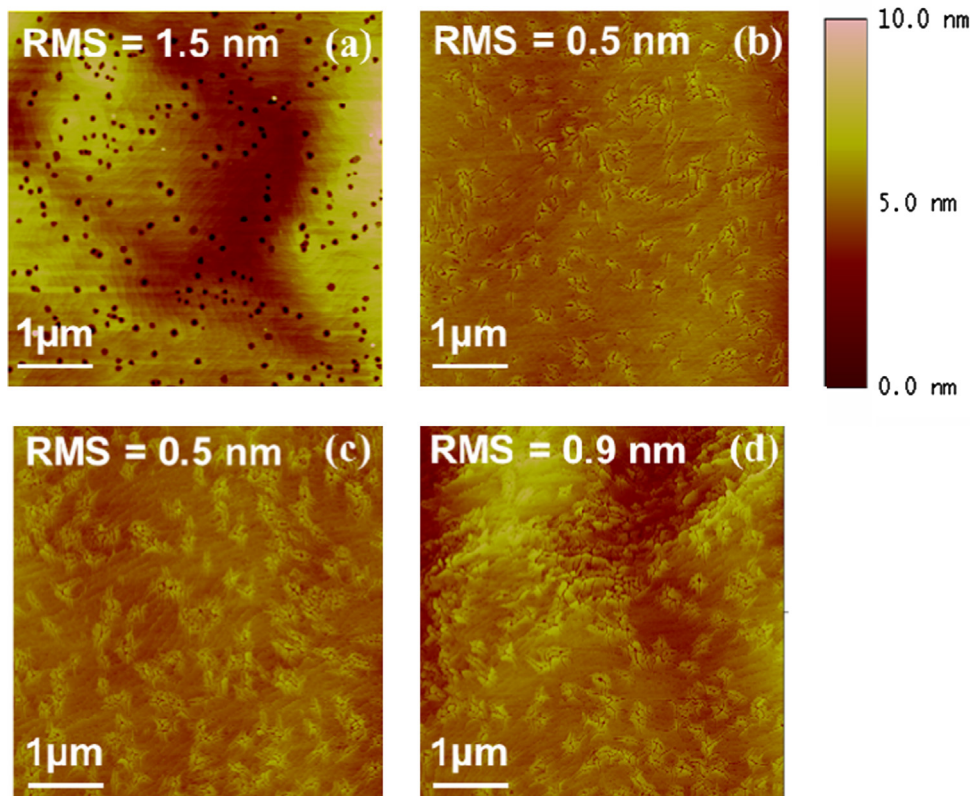


Fig. 3. Surface morphology of (a) LED-epi before HEMT growth, (b) sample A, (c) sample B, and (d) sample C on LEDs.

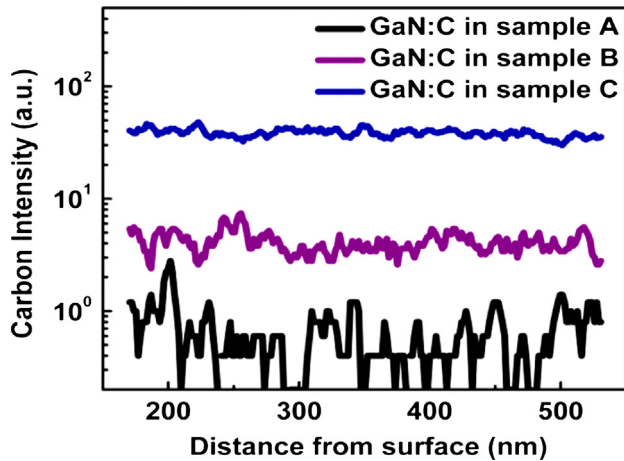


Fig. 4. SIMS results for carbon doping in GaN:C buffer of the three samples on LEDs.

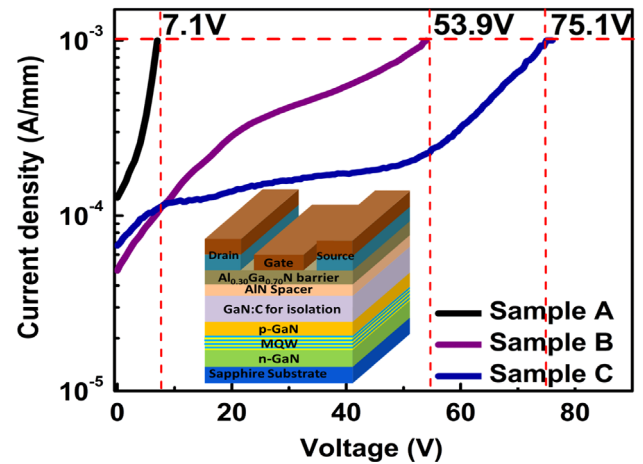


Fig. 6. Off state breakdown characteristics for the three samples on LEDs.

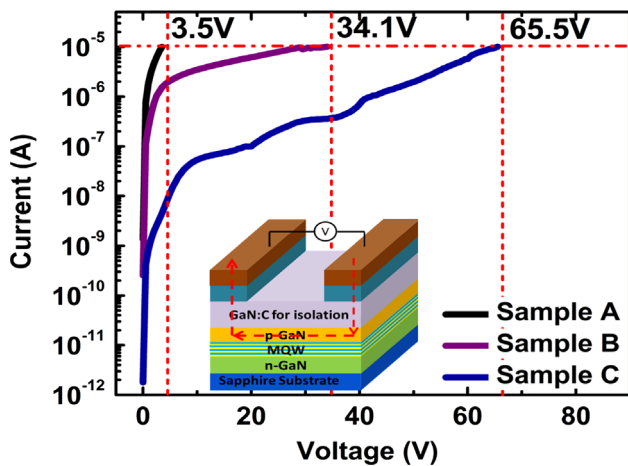


Fig. 5. Buffer breakdown characteristics for the three samples on LEDs.

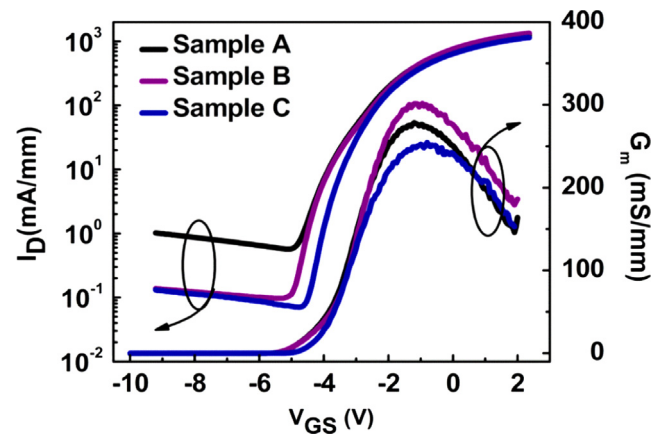


Fig. 7. Transfer curves for the three samples on LEDs.

observed on the surface of the p-type GaN layer, which was intentionally roughened to improve light extraction efficiency [10]. After the HEMT-epi growth the pits disappeared and line-shaped defects emerged for all three samples, as shown in Fig. 3 (b)–(d). The line-shaped defects are related to the underlying pits, originated from threading dislocations and are formed due to the fact that Ga atoms may not have enough energy to migrate to proper sites during the much reduced low temperature p-type layer growth (i.e., 800 °C) [11]. During subsequent HEMT growth at a higher temperature, lateral growth of GaN was enhanced and the pits were filled. In the meantime, line-shaped defects were formed at small-angle boundaries of the slightly misoriented crystal domains [12]. Furthermore, the root-mean-square (RMS) roughness of the LED-epi before HEMT growth was 1.5 nm. After HEMT growth, the RMS values dropped to 0.5 nm, 0.5 nm, and 0.9 nm in sample A, B and C, respectively. The minor increase in RMS value of sample C indicates a slight degradation of surface morphology with decreased V/III ratio.

Fig. 4 illustrates the SIMS results for the HEMT buffer region of the three samples for comparison of relative carbon levels. Negligible carbon doping can be detected in sample A, which is grown under a pressure of 200 mbar with an ammonia flow rate of 4500 sccm. As the growth pressure was lowered to 50 mbar, obvious carbon doping appeared in sample B. With further decreased V/III ratio in sample C, the carbon doping concentration was significantly increased. This agrees well with previous reports that carbon incorporation efficiency increases with reduced reactor

pressure and lower V/III ratio [13]. Carbon is generally incorporated as an acceptor-type electron trapping center in GaN under such conditions. The carbon acceptors compensate the n-type background doping in GaN resulting in semi-insulating GaN epilayers. In addition, the enhanced potential barrier at the subgrain boundaries by heavy carbon doping can also trap carriers and lead to high resistivity [14]. Therefore, improved buffer resistivity and thus enhanced breakdown performance can be anticipated for the samples with increased carbon doping concentration.

To study the influence of carbon doping on buffer resistivity, buffer leakage current of the three HEMT samples versus applied voltages was measured as plotted in Fig. 5. The distance between two metal pads was 100 μm . The two terminal buffer breakdown voltage (V_{BB}) is defined as the measured voltage when the buffer leakage current reaches 10 μA . It could be seen that sample A with negligible intentional carbon doping exhibited poor breakdown characteristics. The relatively thin low quality HEMT buffer grown at a relatively low temperature (920 °C) can result in degraded buffer resistivity [15]. With intentional carbon doping introduced in sample B, V_{BB} was increased by one order of magnitude to 34.1 V. The V_{BB} of sample C, with the highest carbon doping concentration, was as high as 65.5 V. The significantly increased V_{BB} in samples B and C are attributed to the improved buffer resistivity by carbon doping and therefore enhanced isolation from the underlying conductive p-type GaN layer.

The off state breakdown characteristics of the three HEMT samples are plotted in Fig. 6. The off state breakdown voltage

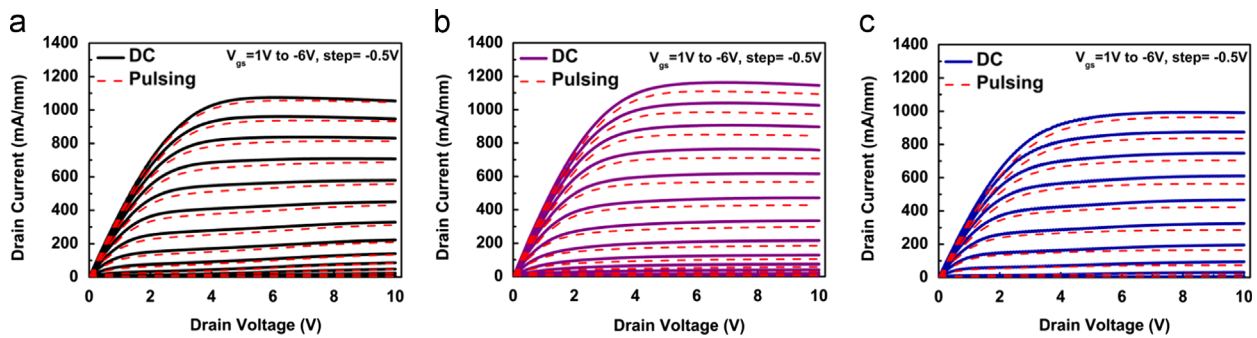


Fig. 8. dc and pulsed output characteristics for (a) sample A, (b) sample B, and (c) sample C on LEDs.

(V_{Boff}) for the HEMTs is defined as the measured voltage when the off state drain current density reaches 1 mA/mm. With the carbon doping concentration increased in the HEMT buffer, the V_{Boff} was increased by an order of magnitude, from 7.1 V in sample A to 75.5 V in sample C. The improved off state breakdown characteristics are mainly attributed to higher buffer resistivity, benefited from carbon doping.

Fig. 7 compares the transfer characteristics of the HEMTs fabricated on the three samples. All three samples showed similar maximum current levels (I_{dss}) of around 1250 mA/mm. It is noticeable that with carbon doping boosted in the regrowth buffer of samples B and C, the off state drain leakage current is also reduced by nearly one order of magnitude, compared to that of sample A. This observation is consistent with improved breakdown characteristics with the carbon doping. In addition, a slight increase of maximum transconductance ($G_{\text{m,max}}$) was observed in sample B. This might be due to the fact that the GaN:C buffer serves as a back barrier which benefits carrier confinement inside the channel region and thus allows a better modulation of the electrons by the gate voltage [16]. With carbon doping further increased, the $G_{\text{m,max}}$ was decreased slightly in sample C. This could be related to the degraded surface morphology with too much carbon doping. The carbon doping concentration can be further optimized to better balanced breakdown characteristics and two-dimensional electron gas (2DEG) conductivity.

Fig. 8(a)–(c) show the dc and pulsed output current–voltage (I – V) characteristics for the three samples. For pulsed measurement, V_{gs} was pulsed from base voltage (-6 V) to the final V_{gs} value, and the pulse width/period was 500 μs /s. As can be noted in Fig. 8(a), nearly no differences exist between dc and pulsed I – V curve, indicating little current collapse in sample A with negligible carbon doping. For sample B with carbon doping introduced, a slight current collapse can be observed. With carbon doping further increased in sample C, current collapse remained at a similar level as that of sample B. The slight current collapse in sample B and sample C mainly originates from the trapping effects induced by carbon dopants in the overgrown HEMT buffer. At a high drain voltage, electrons are injected into the GaN buffer layer and trapped in deep levels. The trapped charge depletes the 2DEG from beneath the GaN channel and results in a reduction in drain current for subsequent V_{ds} traces [17–18].

4. Conclusions

In summary, carbon doping was effectively introduced in the regrowth buffer of HEMTs to improve the breakdown characteristics of the HEMT component selectively grown on LED for the integrated HEMT–LEDs. The effects of carbon doping on the surface morphology, breakdown characteristics, and DC performances

have been investigated. By introducing carbon doping to compensate the background n-type carriers, the boosted breakdown characteristics can be achieved for the HEMTs selectively grown on top of the conductive p-contact layer of the LED wafers, without degradation of the DC characteristics. The improved breakdown performance is mainly attributed to better isolation from the underlying conductive p-GaN by the carbon doped GaN buffers.

Acknowledgments

This work was supported by the Research Grants Council of the Hong Kong Special Administrative Government under the Theme-Based Research Scheme (Grant T23-612/12-R). The authors would like to thank Qiang Li, Yuefei Cai, Xing Lu, Huaxing Jiang and Bei Shi for many helpful discussions and Wilson Tang, as well as the staff of the MCPF & NFF of HKUST for technical support.

References

- [1] K.M. Lau, H.W. Choi, S.W.R. Lee, P.K.T. Mok, J.K.O. Sin, C.P. Yue, W.H. Ki, Cost-effective and eco-friendly LED system-on-a-chip, *China Solid State Light.* (2013).
- [2] Z. Li, J. Waldron, T. Detchprohm, C. Wetzel, R.F.K. Jr., T.P. Chow, Monolithic integration of light-emitting diodes and power metal-oxide-semiconductor channel high-electron-mobility transistors for light-emitting power integrated circuits in GaN on sapphire substrate, *Appl. Phys. Lett.* 102 (2013) 192107.
- [3] Z. Liu, T. Huang, J. Ma, C. Liu, K.M. Lau, Monolithic Integration of AlGaIn/GaN HEMTs on LEDs (HEMT–LEDs) by MOCVD, *IEEE Electron Device Lett.* 35 (2014) 330.
- [4] Z. Liu, J. Ma, T. Huang, C. Liu, K.M. Lau, Selective epitaxial growth of monolithically integrated GaN-based light emitting diodes with AlGaIn/GaN driving transistors, *Appl. Phys. Lett.* 104 (2014) 091103.
- [5] S. Heikman, S. Keller, S.P. DenBaars, U.K. Mishra, Growth of Fe doped semi-insulating GaN by metalorganic chemical vapor deposition, *Appl. Phys. Lett.* 81 (2002) 439.
- [6] C.H. Seager, A.F. Wright, J. Yu, W. Götz, Role of carbon in GaN, *J. Appl. Phys.* 92 (2002) 6553.
- [7] Y.C. Choi, M. Pophristic, B. Peres, H.Y. Cha, M.G. Spencer, L.F. Eastman, High breakdown voltage C-doped GaN-on-sapphire HFETs with a low specific on-resistance, *Semicond. Sci. Technol.* 22 (2007) 517.
- [8] J.B. Webb, H. Tang, S. Rolfe, J.A. Bardwell, Semi-insulating C-doped GaN and high-mobility AlGaIn/GaN heterostructures grown by ammonia molecular beam epitaxy, *Appl. Phys. Lett.* 75 (1999) 953.
- [9] Y. Ohba, A. Hatano, A study on strong memory effects for Mg doping in GaN metalorganic chemical vapor deposition, *J. Cryst. Growth.* 145 (1994) 214.
- [10] L.W. Wu, S.J. Chang, Y.K. Su, R.W. Chuang, Y.P. Hsu, C.H. Kuo, W.C. Lai, T.C. Wen, J.M. Tsai, J.K. Sheu, $\text{In}_{0.23}\text{Ga}_{0.77}\text{N}/\text{GaN}$ MQW LEDs with a low temperature GaN cap layer, *Solid State Electron.* 47 (2003) 2027.
- [11] Y.J. Lee, H.C. Kuo, T.C. Lu, S.C. Wang, High light-extraction GaN-based vertical LEDs with double diffuse surfaces, *IEEE J. Quantum Electron.* 42 (2006) 1196.
- [12] H. Sasaki, S. Kato, T. Matsuda, Y. Sato, M. Iwami, Seikoh Yoshida, Investigation of surface defect structure originating in dislocations in AlGaIn/GaN epitaxial layer grown on a Si substrate, *J. Cryst. Growth.* 298 (2007) 305.
- [13] D.D. Koleske, A.E. Wickenden, R.L. Henry, M.E. Twigg, Influence of MOVPE growth conditions on carbon and silicon concentrations in GaN, *J. Cryst. Growth.* 242 (2002) 55.

- [14] H. Tang, J.B. Webb, J.A. Bardwell, S. Raymond, J. Salzman, C. Uzan-Saguy, Properties of carbon-doped GaN, *Appl. Phys. Lett.* 78 (2001) 757.
- [15] S. Strite, H. Morkoç, GaN, AlN, and InN: a review, *J. Vac. Sci. Technol. B.* 10 (1992) 1237.
- [16] T. Palacios, A. Chakraborty, S. Heikman, S. Keller, S.P. DenBaars, U.K. Mishra, AlGaIn/GaN high electron mobility transistors with InGaIn back-barriers, *IEEE Electron Device Lett.* 27 (2006) 13.
- [17] S.C. Binari, P.B. Klein, T.E. Kazior, Trapping effects in GaN and SiC microwave FETs, *Proc. IEEE* 9 (2002) 1048.
- [18] S.C. Binari, K. Ikossi, J.A. Roussos, W. Kruppa, P. Doewon, H.B. Dietrich, D.D. Koleske, A.E. Wickenden, R.L. Henry, Trapping effects and microwave power performance in AlGaIn/GaN HEMTs, *IEEE Trans. Electron Devices* 48 (2001) 465.